이학석사 학위논문

Fabrication of Graphene Quantum Dots from Chemical Vapor Deposited Graphene using Gold-incorporated Micelles as Etching Mask

금을 도입한 마이셀을 에칭마스크로 사용한 화학증착그래핀에서 그래핀양자점의 제조

2016년 8월

서울대학교 대학원
화학부 고분자화학 전공
이 정 섭

Fabrication of Graphene Quantum Dots from Chemical Vapor Deposited Graphene using Gold-incorporated Micelles as Etching Mask

지도교수 손 병 혁

이 논문을 이학석사 학위논문으로 제출함

2016년 6월

서울대학교 대학원

화학부 고분자화학 전공

이 정 섭

이정섭의 이학석사 학위논문을 인준함

2016년 6월

위 원 장 김 경 택 (인)

부위원장 손 병 혁 (인)

위 원 정 택 동 (인)

Abstract

Fabrication of Graphene Quantum Dots from Chemical Vapor Deposited Graphene using Gold-incorporated Micelles as Etching Mask

Chung Sub Lee
Department of Chemistry
The Graduate School
Seoul National University

Graphene quantum dots (GQDs) are nano-sized graphene of a single layer or a few layers, with many unique optical, mechanical, and photoelectric properties induced by the quantum confinement effect and edge effect. Well-known techniques to prepare GQDs include electron beam lithography, chemical synthesis, graphene oxide reduction, and hydrothermal methods. We aimed in the present study to synthesize GQDs from the self-assembly of diblock copolymers. Diblock copolymer forms micelles in selective solvents. Polystyrene-*block*-poly(4-vinylpyridine) (PS-P4VP) block copolymer was used for nanostructure self-assembly, as metal precursors can be incorporated into the P4VP block. Block copolymer micelles were annealed with solvent vapor to fabricate cylindrical

nanostructures on various substrates. Metal nanostructures were synthesized from metal-incorporated block copolymer nanostructures by oxygen plasma. The synthesized metal nanoparticles were used as etching masks to fabricate GQDs. We characterized the GQDs by Raman spectroscopy. Based on our observations, we speculated that various large-scale graphene nanostructures of well-defined geometry will be easily accessible for semiconductor applications.

Keywords: Diblock copolymer, Self-assembly, Graphene quantum dots, Raman spectroscopy

Student number: 2014-22409

Contents

List of Figures

Chapter 2. Metal nanostructures from directed self-assembly of diblock copolymers on confined substrates

Chapter 3. Fabrication of GQDs from CVD graphene using gold-incorporated micelles as etching mask

Chapter 1

Background

1.1. Self-assembly of diblock copolymer

Diblock copolymer is a combination of two homopolymers connected by a covalent bond. Many scientists are concerned with the microphase separation of block copolymers [1], as it results in large-area nanoscale patterns, which is hard to achieve by other methods. The microphase separation of diblock copolymers depends on three parameters: the volume fractions of the two blocks, the total degree of polymerization, and the Flory–Huggins parameter which is a parameter of incompatibility between the two blocks [2]. In most cases, interactions between different blocks are much less favorable than those between the same blocks.

Diblock copolymers microphase separate into a variety of morphologies, including spheres, cylinders, gyroids, and lamellae. Owing to the tunability of the size, shape, and composition of diblock copolymers, they are attractive for nanotechnology applications [3, 4]. Block copolymers are used in various areas such as fabrication of masks and pores, nanoparticle synthesis, and nanomaterial templating [5].

Block copolymers have high potential in lithography, as they self-assemble into patterns smaller than other current techniques can achieve. These patterns are also available in thin films, which make it available for semiconductor productions. In lithography, a great deal of difference in etching rate is required to transfer the block copolymer patterns onto substrates [6]. Polymethylmethacrylate (PMMA) is an example for selective etching in UV light [7]. For oxygen plasma, a widely used technique for low-temperature etching, inorganic molecules are introduced into block copolymers for selectivity. Polydimethylsiloxane (PDMS) is a case that the block itself has an inorganic atom [8]. Polyvinylpyridine (PVP) has nitrogen atom that can be quaternized so that the block has positive charges to attract

anions. Heavy-atom precursors such as gold chloride or platinum tetrachloride can interact with PVP, thus incorporating metal into the block copolymer nanostructure [9, 10]. Upon oxygen plasma, inorganic atoms retain the morphology of the selected block, which is used for further treatments.

1.2. Graphene nanostructures and graphene quantum dots (GQDs)

Graphene is a two-dimensional planar material that is one atom thick with a honeycomb lattice of carbon atoms. Since the first report of simple preparation by mechanical exfoliation [11], a large number of studies have revealed significant features of graphene such as mechanical strength [12], high thermal conductivity [13], and electron mobility [14].

One of the unique property of graphene is that it is a zero-gap semiconductor, as the conduction and valence bands meet on certain points, named Dirac points [15]. For optoelectronic applications, people have sought to generate a discrete band gap which is possible by controlling the shape of graphene. Various methods such as lithography, nanoimprinting, and chemical techniques have been used to fabricate graphene nanoribbon (GNR) [16], graphene nanomesh (GNM), and GQDs [17]. Extraordinary properties of nanostructured graphenes, which pristine graphene does not show, have been widely explored.

Mass production of graphene in large quantities at lower costs compared to existing materials is essential for further application of graphene and its nanostructures. Currently, there are many techniques for graphene productions. Many investigators tried to exfoliate graphene from graphitic materials. Mechanically, shearing and sonication methods were intensively studied. On the other hand, rather than such top-down methods

mentioned above, some people thought of graphene from carbon atoms. Recently chemical vapor deposition (CVD) has been spotlighted as an important method for the preparation and production of graphene [18]. Methane gas is primarily used for the source of carbon atoms to synthesize graphene on metal surfaces [19].

1.3. References

[1] Y. Mai, A. Eisenberg, *Chem. Soc. Rev.*, **2012**, *41*, 5969–5985.

[2] F. S. Bates, G. H. Fredrickson, *Phys. Today*, **1999**, *52*, 32–38.

[3] I. W. Hamley, *Nanotechnology* **2003**, *14*, R39–54.

[4] M. Lazzari, M. A. López-Quintela, *Adv. Mater.* **2003**, *15*, 1583–94.

[5] S. B. Darling, *Prog. Polym. Sci.* **2007,** *32*, 1152–1204.

[6] L. A. Ponomarenko, F. Schedin, M. I. Katsnelson, R. Yang, E. W. Hill, K. S. Novoselov, A. K. Geim, *Science*, **2008**, *320*, 3568.

[7] M.-S. Seo, J.-H. Kim, S.-S. Kim, H. J. Kang, B.-H. Sohn, *Nanotechnology*, **2015**, *26*, 165302.

[8] J. G. Son, K. W. Gotrik, C. A. Ross, *ACS Macro Lett.*, **2012**, *1*, 1279–1284.

[9] S.-S. Kim, B.-H. Sohn, *RSC Adv.*, **2016**, *6*, 41331-41339.

[10] S.-S. Kim, M. J. Park, J.-H. Kim, G. H. Ahn, S. M. Ryu, B. H. Hong, B.-H. Sohn, *Chem. Mater.*, **2015**, *27*, 7003–7010.

[11] K. S. Novoselov, A. K. Geim, S. V. Morozov, D. Jiang, Y. Zhang, S. V. Dubonos, I. V. Grigorieva, A. A. Firsov, *Science* **2004**, *306*, 666−669.

[12] C. G. Lee, *Science* **2008**, *321*, 385–388.

[13] A. A. Alandin, S. Ghosh, W. Bao, I. Calizo, D. Teweldebrhan, F. Miao, C. N. Lau, *Nano Lett.* **2008**, *8*, 902–907.

[14] A. K. Geim, K. S. Novoselov, *Nature Mater.* **2007**, *6*, 183–191.

[15] K. S. Novoselov, A. K. Geim, S. V. Morozov, D. Jiang, M. I. Katsnelson, I. V. Grigorieva, S. V. Dubonos, A. A. Firsov, *Nature* **2005**, *438*, 197-200.

[16] M. Y. Han, B. Ozyilmaz, Y. B. Zhang, P. Kim, *Phys. Rev. Lett.* **2007**, *98*, 206805.

[17] J. Lee, K. Kim, W. I. Park, B. H. Kim, J. H. Park, T. H. Kim, S. Bong, C. H. Kim, G. Chae, M. Jun, Y. Hwang, Y. S. Jung, S. Jeon, *Nano Lett.* **2012**, *12*, 6078−6083.

[18] Y. Zhang, L. Zhang, C. Zhou**,** *Acc. Chem. Res.* **2013**, *46*, 2329–2339.

[19] L. G. De Arco, Y. Zhang, A. Kumar, C. Zhou, *IEEE Trans. Nanotechnol.* **2009**, *8*, 135–138.

Chapter 2

Metal nanostructures from directed self-assembly of diblock copolymers on confined substrates

2.1. Introduction

Microphase segregation of block polymers is a thermodynamically driven process that leads to nanoscale periodic structures. The most practical applications of self-assembled block polymers rely on thin film formation since this is the most appropriate form to create a surface pattern that can be transferred to a substrate for the creation of functional nanoscale devices [1, 2].

Block polymer thin films cast from a solvent onto a substrate are likely to be kinetically trapped in non-equilibrium, resulting in disorganized structures. The mobility of the polymer chains must be sufficient to allow for structural reorganization into the highly regular structures predicted for equilibrium. Thermal treatments above the glass transition temperature (Tg) of the system can anneal the polymer to the equilibrium structure [3]. However, for many high molar mass systems, very long annealing times are required to achieve large-area ordering of nanostructures, making the whole process inefficient [4].

Against such time-consuming process, another annealing technique known as solvent vapor annealing (SVA) has gained interest [5]. Block polymer thin films are exposed to vapors of one or more solvents. The solvent vapor swells the polymer film, giving mobility to the polymer chains. On subsequent solvent evaporation, polymer chains find a more stable conformation to form a well-organized nanostructure [6].

To control the morphology of the block copolymer nanostructure even further, scientists modified the surface energy state of the polymer thin film chemically or physically. Such edges epitaxially affected a large area of the thin film to guide the morphology of the thin films to their use [7, 8].

In this study, we facilitated SVA to fabricate cylindrical block copolymer nanostructure from a thin film of diblock copolymer micelles on flat and stripe-patterned substrates. The pattern successfully guided the block copolymer morphology into long-range parallel cylinders, which would have been randomly arranged without the pattern. A parallel array of Pt nanowires was obtained from the guided block copolymer cylinders.

2.2. Materials and Methods

2.2.1. Fabrication of cylindrical nanostructures by Solvent Vapor Annealing

A silicon substrate with a thermally grown oxide layer (300 nm in thickness) was cleaned by piranha solution (70/30 v/v concentrated H_2SO_4 and 30% H_2O_2), thoroughly rinsed with deionized water, and dried with nitrogen. Polystyrene-*block*-poly(4-vinylpyridine) (PS-P4VP), whose average molecular weight (Mn, kg/mol) is 32k-13k and polydispersity index (PDI) is 1.08, was purchased from Polymer Source Inc. It was dissolved in toluene to a concentration of 0.6 wt%. The solution was stirred for 3 hrs at 85˚C and cooled down to room temperature. As toluene is a selective solvent for PS, micelles with PS corona and P4VP core was self-assembled in toluene. This PS-P4VP micellar solution was spin-coated onto a cleaned flat SiO_2/Si substrate, which was exposed to saturated chloroform solvent vapor in a closed glass vessel at room temperature for 5-20 mins. After solvent vapor annealing, the samples were placed under ambient conditions and dried.

2.2.2. Fabrication of well-aligned Pt Nanowires on patterned substrate

The periodic linear pattern (width, 500 nm; periodicity, 1 μm) was fabricated on a layer of photoresist deposited onto SiO_2 (300 nm)/Si wafer using a stepper (Nikon, NSR-2005i10C). CF4 reactive ion etching generated arrays of linear trenches with the depth of approximately 40 nm in the wafer. The PS(32)-P4VP(13) micellar solution was then spin-coated onto the patterned SiO_2/Si substrate, followed by chloroform vapor annealing for 2 hrs. The substrates were then dipped into an acidic Pt salt solution (18 mL of 20 mM Na_2PtCl_6(aq) + 2 mL of 1% HCl(aq)) to load the Pt precursor into the cylindrical P4VP blocks selectively. After immersion for 2 hrs, the substrates were removed and dried under a nitrogen stream, followed by treatment with oxygen plasma for 5 mins (100 W, 38 mTorr) to remove the copolymers and synthesize the nanowires.

2.2.3. Visualization of block copolymer cylindrical morphology

On field emission-scanning electron microscope (FE-SEM), the P4VP cylinders are hidden under the PS phase. The substrates are dipped into ethanol and heated at 50˚C for 30 mins. Ethanol selectively swells the P4VP block. Heat assists the surface reconstruction to reveal the swollen P4VP cylinders, which can be seen with the SEM.

2.3. Results and Discussion

In the present study, we fabricated platinum nanowires from block copolymer nanostructures aligned by Graphoepitaxy on patterned substrates [9]. Block copolymer morphology was primarily determined by the volume fraction of each block [10]. PS(32k)-P4VP(13k) is one of the well-known compositions of the cylinder-forming block copolymer. However, as it assembled into micelles in toluene, it stayed kinetically trapped upon spin-coating (Fig. 2.1.a). This PS-P4VP thin film on patterned substrates was annealed with chloroform, a non-selective solvent for both blocks of PS-P4VP, to form cylindrical nanostructure (Fig. 2.1.b). Pt nanowires were fabricated by incorporating Pt precursors into the cylindrical P4VP (Fig. 2.1.c), followed by oxygen plasma process to remove the polymer and simultaneously reduce the precursor (Fig. 2.1d).

We checked the morphological changes of PS-P4VP on a flat SiO_2/Si substrate to observe the SVA effect. We could easily induce the cylindrical morphology on a flat substrate. Even after 5 mins of annealing, we could observe the cylindrical morphology (Fig. 2.2.a). When we increased the annealing time, we could observe the correlation between the annealing time and the grain size of the cylindrical pattern to some extent (Fig. 2.2.b). The distance between the cylinders was measured as 38-39 nm.

The same conditions were applied to the patterned substrate. We found that both trench depth and annealing time affected the quality of the cylinder alignments [11, 12]. We also observed the case where cylinders were ordered perpendicular to the substrate surface rather than parallel to it; other investigators suggested that this phenomenon might be produced when the film was slightly thicker than the thickness we intended for parallel

cylinders [13]. We have successfully optimized the specific combination of experimental conditions to induce parallel cylinders shown in Fig. 2.3.a. For example, 0.6wt% PS-P4VP(32k-13k) toluene solution was spin-coated (4000 rpm, 1 min) on the 40nm-patterned substrate, when the optimal annealing time proved to be 2 hrs. A slight variation in inter-cylindrical distance was observed, which might be caused by the interaction between the polymer film and trench walls during the process of swelling and shrinkage [14]. Pt precursors were incorporated into the cylinders by submerging the substrate into acidic platinum hexachloride solution. After 2 hrs, all polymers were removed by oxygen plasma. Consequently, reduced Pt nanowires were formed on the substrate (Fig. 2.3.b). Based on our observation, 2-13 nanowires were present in each 500 nm trench. And we found that the distance between the nanowires was comparable to that between the cylinders on the flat surface.

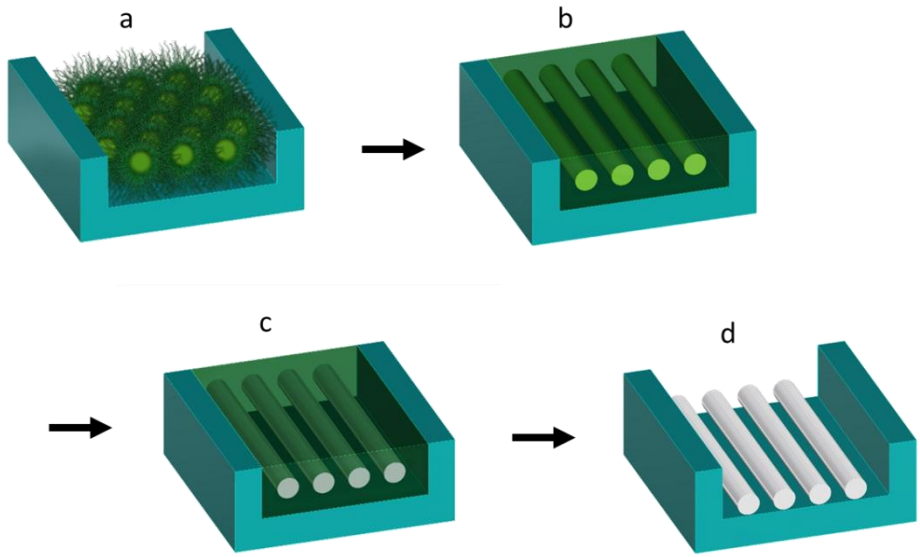

Figure 2.1. Schematic representation of Pt nanowire fabrication. (a) Micelles are spin-coated on a patterned substrate. (b) Cylindrical morphology achieved by solvent vapor annealing. (c) Pt precursors are incorporated into the cylinder core. (d) Oxygen plasma removes the polymer and Pt nanowire is fabricated.

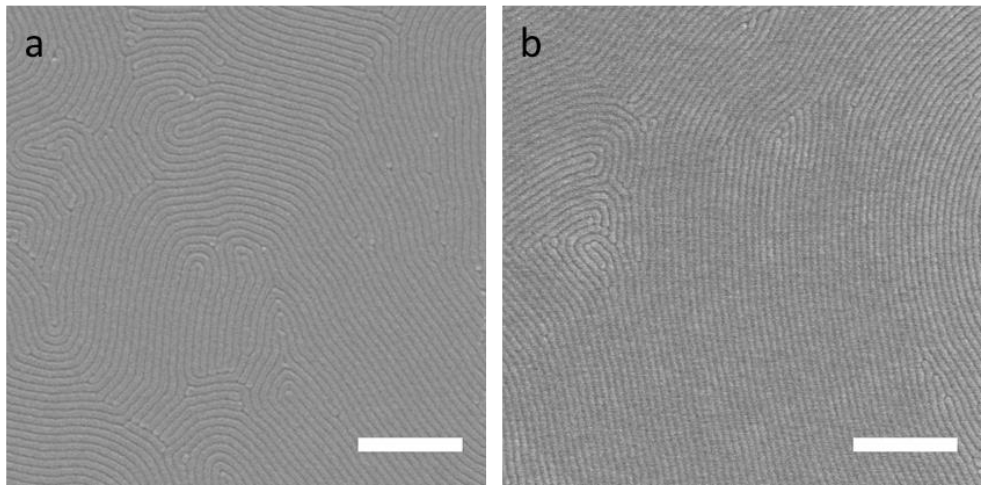

Figure 2.2. SVA of PS-P4VP (32k-13k) on flat surface for 5 mins (a) and 20 mins (b). Scale bars are 500 nm.

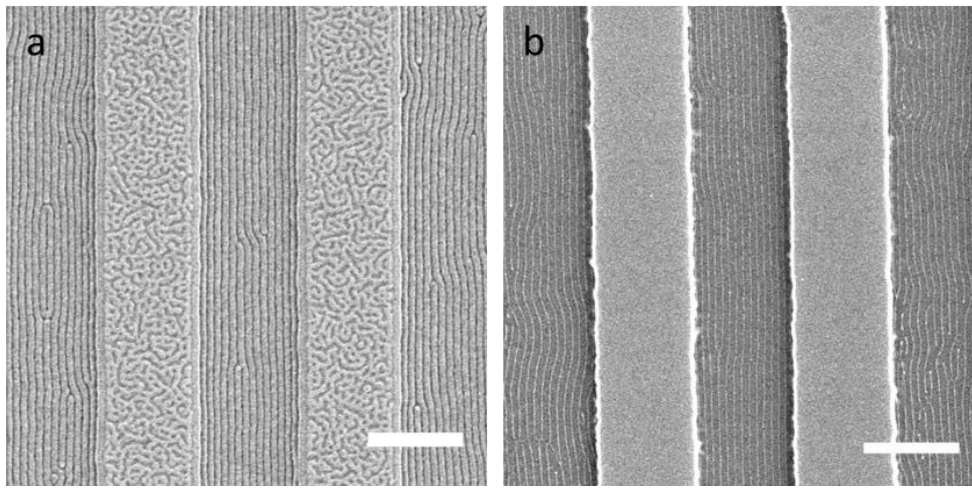

Figure 2.3. SEM images of well-aligned PS-P4VP (32k-13k) cylinders on patterned SiO_2/Si (a) and Pt nanowires from well-aligned PS-P4VP (32k-13k) cylinders (b). Scale bars are 500 nm.

2.4. References

[1] M. P. Stoykovich, P. F. Nealey, *Materials Today*, **2006**, *9*, 20.

[2] R. A. Segalman, et al. *Macromolecules*, **2009**, *42*, 9205.

[3] T. P. Russell, R. P. Hjelm, P. A. Seeger, *Macromolecules*, **1990**, *23*, 890−893.

[4] J. Chai, D. Wang, X. Fan, J. M. Buriak, *Nat. Nanotechnol.* **2007**, *2*, 500.

[5] X. Gu, I. Gunkel, A. Hexemer, T. P. Russell, *Colloid Polym. Sci.* **2014**, *292*, 1795−1802.

[6] S.-M. Jeon, S. H. Lee, S. I. Yoo, B.-H. Sohn, *Langmuir* **2011**, *27*, 12191.

[7] M. Luo, T. H. Epps III, *Macromolecules* **2013**, *46*, 7567–7579.

[8] S.-S. Kim, B.-H. Sohn, *Carbon* **2016**, *In press.*

[9] J. Chai, D. Wang, X. Fan, J.M. Buriak, *Nat. Nanotechnol.*, **2007**, *13*, 500–506.

[10] R. A. Segalman, *Materials Science and Engineering*, **2005**, *R 48*, 191–226.

[11] S. Kim, D. O. Shin, D.-G. Choi, J.-R. Jeong, J. H. Mun, Y.-B. Yang, J. U. Kim, S. O. Kim, J.-H. Jeong, *Small*, **2012**, 8, 1563–1569.

[12] P. W. Majewskia, K. G. Yager, *Soft Matter*, **2016**, *12*, 281-294.

[13] X. Zhang, B. C. Berry, K. G. Yager, S. C. Kim, R. L. Jones, S. Satija, D. L. Pickel, J. F. Douglas, A. Karim, *ACS Nano*, **2008**, *2*, 2331-2341.

[14] C. Cummins, A. Gangnaik, R. A. Kelly, D. Borah, J. O'Connell, N. Petkov, Y. M. Georgiev, J. D. Holmes, M. A. Morris, *Nanoscale*, **2015**, *7*, 6712-6721.

Chapter 3

Fabrication of GQDs from CVD graphene using gold-incorporated micelles as etching mask

3.1. Introduction

GQDs are very small pieces of graphene with the diameter less than 20nm [1]. Due to its near-0D quantum confinements, the GQDs exhibit some characteristics similar to carbon dots as well as the physical properties of graphene [2]. Most importantly, the band gap of the GQDs can be manipulated by chemical modifications and size control [3]. GQDs are also highly photo-stable compared to organic dyes and semi-conductive quantum dots [4]. GQDs' low toxicity and biocompatibility make them a promising candidate for biosensor applications [5].

Various techniques have been developed to prepare GQDs, including top-down methods such as hydrothermal cutting [6] and graphene oxide reduction [7], along with bottom-up chemical synthetic methods [8]. While most top-down methods suffer from lack of size control [9], block copolymer lithography has its strength in nanoscale patterning owing to the long-range ordering of block copolymer morphology. Thus it is a potential route to the well-defined large-area fabrication of GQDs. Recently, the synthesis of 10 and 20nm GQDs by BCP nanospheres was reported [10].

We aimed in the present study to produce sub-10nm sized GQDs arrayed on a silicon substrate by applying self-assembled block copolymer micelles directly onto CVD graphene. The micelle core was loaded with gold precursors to give etching contrast for GQDs. The size and distance of GQDs were controlled by changing the molecular weight of the block copolymer. The GQDs were characterized with Raman spectroscopy, showing potential use for further applications.

3.2. Materials and Methods

3.2.1. Solution of Au-incorporated PS-P4VP micelles

Three PS–P4VP diblock copolymers of different molecular weights (Mn: 33k–8k, PDI =1.06; Mn: 51k–18k, PDI = 1.15; Mn: 109k–27k, PDI = 1.15) were purchased from Polymer Source Inc. PS-P4VP (0.01g) was dissolved in chloroform (4g), a fairly non-selective solvent for both blocks. Toluene (2g) was slowly added by a syringe pump to this mixture at a rate of 3.0 ml/hr to induce the formation of micelles. After mixing, chloroform was evaporated under reduced pressure and the solution was diluted with toluene to obtain desired concentration. $HAuCl_4$, a precursor of Au nanoparticles, was added to the micellar solution. The solution was stirred for at least seven days at room temperature.

3.2.2. Fabrication of GQDs

CVD graphene on SiO_2/Si was purchased from Graphene Square. A single layer of Au-incorporated PS–P4VP micelles was spin-coated (typically at 2000 rpm, 60 sec) on the substrate covered with graphene. The block copolymer micellar array was treated with oxygen plasma (100 W, 38 mTorr) for 3 mins. The product was submerged in aqua regia (a concentrated mixture of HCl and HNO_3) for 30 mins to reveal the graphene quantum dots under the Au nanoparticles.

3.2.3. Characterization

Nanostructures were analyzed using an atomic force microscope (AFM) with a Multimode 8 AFM and a Nanoscope V controller (Bruker) in tapping mode with Al-coated Si cantilevers. X-ray photoelectron spectroscopy (XPS) was performed using a Sigma Probe (Thermo VG) with a monochromatic Al Kα x-ray source operating at 100 W. Raman spectra were obtained using a Renishaw 2000 with a 514.5 nm line from an Ar ion laser as an excitation source.

3.3. Results and Discussion

For fabrication of GQDs by using Au-incorporated micelles as etching mask, we adopted PS-P4VP of three different molecular weights (Mn=33k-8k, 51k-18k, 109k-27k), whose procedures were represented in Fig 3.1. PS-P4VP solution was carefully prepared for narrow distribution in micelle size. We chose $HAuCl_4$ as a precursor for Au nanoparticle, which was incorporated into micelles by vigorous stirring. The Au-incorporated micelles were directly spin-coated on CVD graphene. Oxygen plasma treatment was applied to remove the polymer and to reduce metal precursors into nanoparticles. CVD graphene was also etched, but the etch rate difference induced by the metal precursors resulted in the protection of graphene right beneath the synthesized Au nanoparticles. Finally, we applyed aqua regia to selectively remove the Au nanoparticles, and thus finally to obtain the GQD arrays.

Before applying the Au-incorporated micelles onto CVD graphene, we attempted to determine the appropriate concentration and spin-coating

speed of BCP micelles for single-layer hexagonal arrays on SiO_2/Si. This procedure was necessary to ensure that there were no micelle double-layers on the graphene. We observed hexagonal arrays of block copolymer micelles on the SiO_2/Si substrate (Fig. 3.2.a-c) by spin-coating (1 min, 2000 rpm) 0.1wt% , 0.15wt%, 0.2wt% solutions of PS-P4VP with different molecular weights of Mn=33k-8k, 51k-18k, 109k-27k, respectively. Although a single layer of micelles was spin-coated, the micelles did not exhibit a well-aligned hexagonal array following their application onto graphene (Fig. 3.2.d-f). The surface energy difference between the two materials might be the key factor to this disruption. It is well known that graphene surface is hydrophobic [11], whereas SiO_2/Si cleaned with piranha solution is hydrophilic due to the surface hydroxyl groups [12, 13].

In a subsequent experiment, oxygen plasma was applied to remove excess CVD graphene (Fig 3.3.a-c). Upon its application, PS-P4VP micelles were removed, while the Au nanoparticles were synthesized from $HAuCl_4$, which served as an etching mask for the underlying graphene [14].

Finally, Au nanoparticles were removed by aqua regia and the GQDs were revealed (Fig. 3.4). The AFM images showed that the size and spatial density of GQDs corresponded to those of the Au nanoparticles. We measured the height profile of the GQDs, which was quite regular. The height of the GQDs was approximately 0.7nm in the three cases, which was consistent with the previous studies [10].

The removal of Au nanoparticles was confirmed by XPS measurement (Fig. 3.5). Before the aqua regia treatment, two characteristic peaks from the doublet state of Au 4f orbitals were observed. Au

nanoparticles were mostly in reduced state, since we did not observe the gold oxide doublet peaks which would have appeared +2ev shifted from Au^0 doublet [15, 16]. After aqua regia treatment, we can confirm the removal of Au nanoparticles by the disappearance of those peaks, which was distinct before aqua regia treatment.

Finally, we measured the Raman spectrum of the CVD graphene and GQDs on SiO_2/Si (Fig. 3.6). It has been well established that CVD graphene exhibited the typical D, G, and 2D peaks (Fig. 3.6.a) [10, 17]. In the GQD Raman spectrum, the D peak was slightly wider than the G peak, and the 2D peak was not visible (Fig. 3.6.b). This indicates the decrease in the number of sp^2 –bonding carbons, as it is a sequence of GQD fabrication from CVD graphene. We observed another small peak between D and G peaks. This might be a characteristic peak of fullerene, which has distorted sp^2 bonds [17]. It has been reported that small-size (i.e., less than about 20nm) graphene is relatively unstable [18, 19]. We assumed that this transformation might have been facilitated by oxygen plasma at the edges.

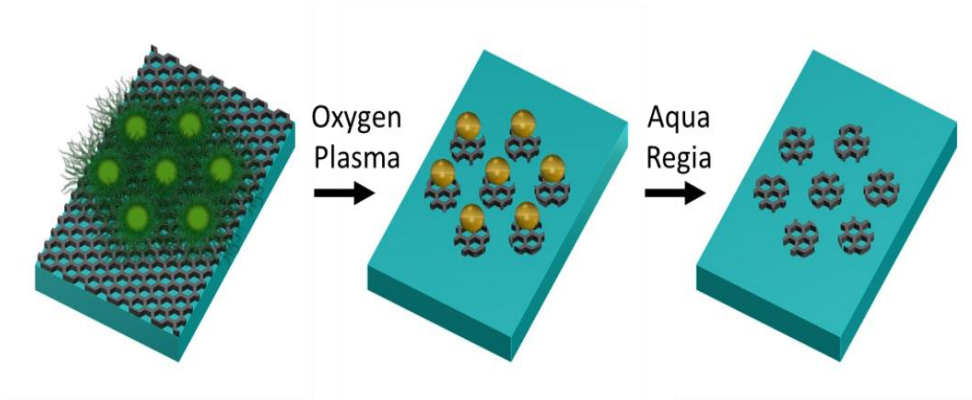

Fig. 3.1. Schematic representation of GQD fabrication.

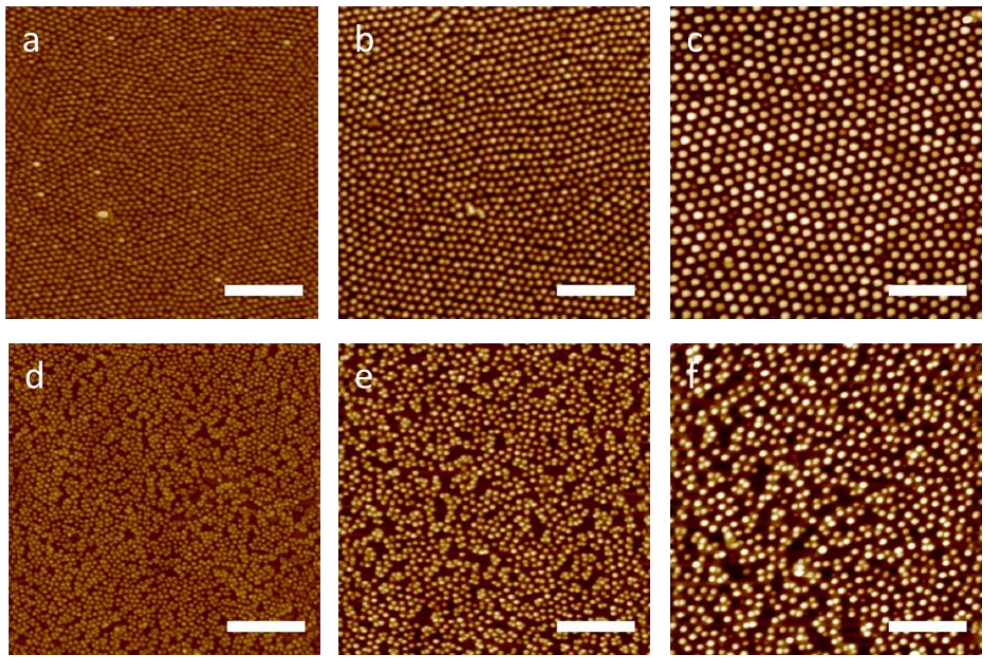

Fig 3.2. Micelles spin-coated onto bare SiO_2/Si (a-c) and CVD graphene (d-f). Concentrations and Molecular weights of the polymers were (a,d) 0.1wt% PS(33k)-P4VP(8k), (b,e) 0.15wt% PS(51k)-P4VP(18k), and (c,f) 0.2wt% PS(109k)-P4VP(27k). Scale bars are 500nm.

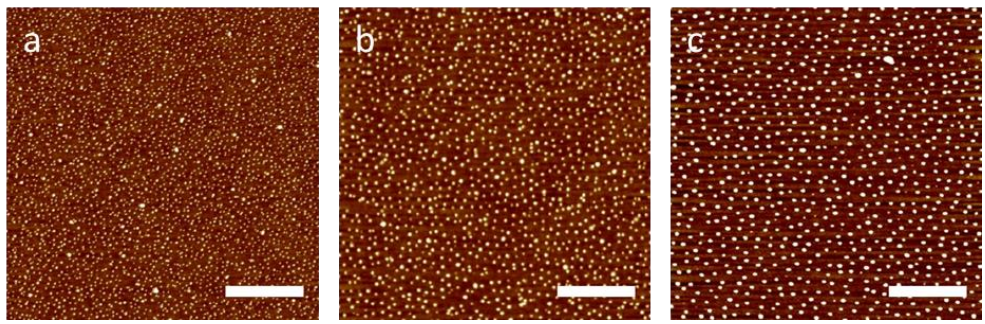

Fig 3.3. Au nanoparticles from PS-P4VP micelles (a, 33k-8k; b, 51k-18k; c, 109k-27k). Scale bars are 500nm.

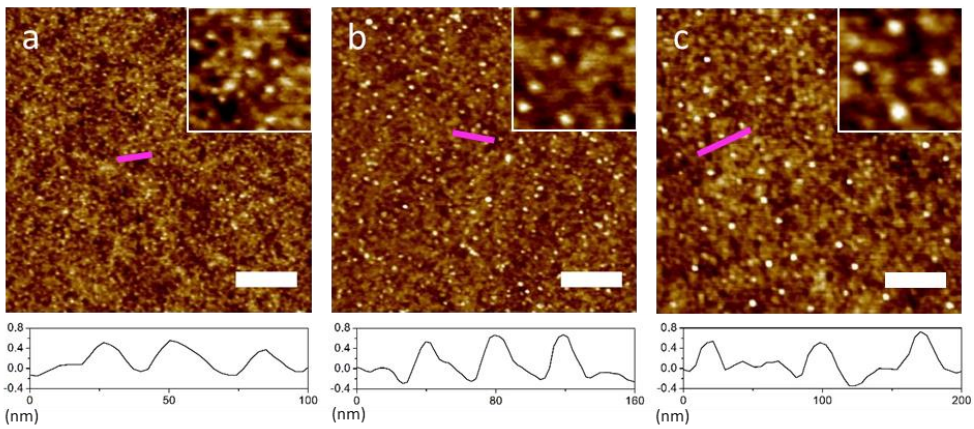

Fig 3.4. AFM images of the GQDs from PS-P4VP micelles (a, 33k-8k; b, 51k-18k; c, 109k-27k) revealed by aqua regia treatment. Height profile along the pink line is shown under each AFM image. Insets in a-c represent magnified views of GQDs. Scale bars are 200nm.

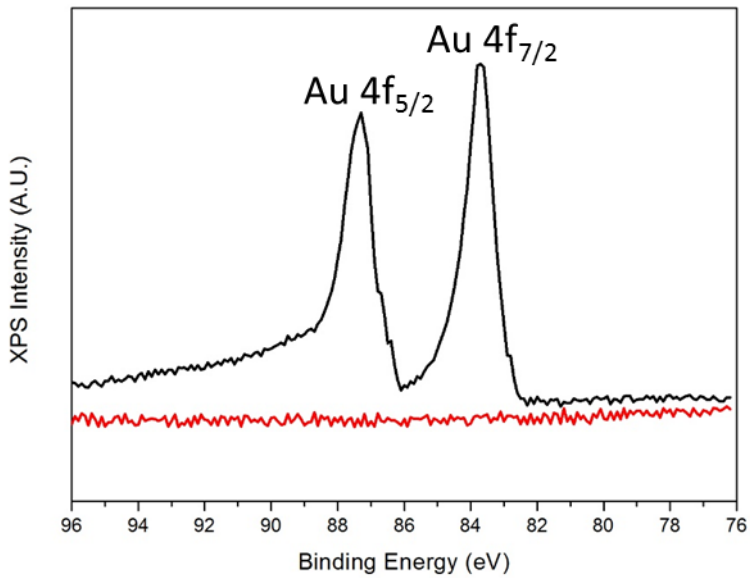

Fig 3.5. XPS spectrum of Au atom (4f) before (black line) and after (red line) aqua regia treatment.

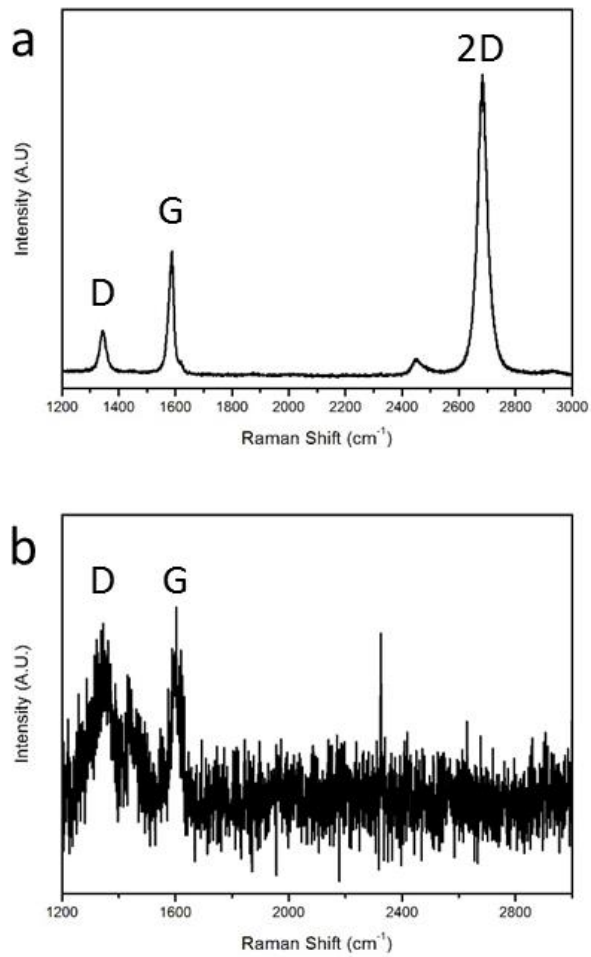

Fig 3.6. Raman spectra of CVD graphene (a) and GQDs (b).

3.4. Summary and Prospective studies

The present study showed that block copolymer self-assembly and its nanostructures could be utilized for inorganic templates, which might be applied for nanolithography of graphene. PS-P4VP diblock copolymer was applied for nanolithography. The morphology of block copolymers could be controlled by solvent vapor annealing on flat or patterned substrates. Block copolymer nanostructures could also be utilized as templates for inorganic nanostructure. Inorganic materials were adopted at various stages of the lithography process. The inorganic nanostructure was used as an etching mask for fabricating GQDs from CVD graphene.

Applications of GQDs require further characterization and numerous modifications. However, most applications require large-scale production of GQDs. Although CVD graphene is excellent in quality, it is still not easily accessible as it requires sophisticated procedures for production. It is also notable that the production of multilayer (approximately three to ten layers) graphene is inefficient with CVD methods. Multilayer graphene nanostructures can be efficiently fabricated from exfoliated graphenes. The combination of exfoliation methods and current nanolithography techniques will be further explored in our

laboratory for the future studies.

3.5. References

[1] M. Bacon, S. J. Bradley, T. Nann, *Part. Part. Syst. Charact.*, **2014**, *31*, 415–428.

[2] J. shen, Y. Zhu, X. Yang, C. Li, *Chem. Commun.*, **2012**, *48*, 3686-3699.

[3] L. Li, G. Wu, G. Yang, J. Peng, J. Zhao, J.-J. Zhu, *Nanoscale*, **2013**, *5*, 4015-4039.

[4] H. J. Sun, L. Wu, W. Wei, X. Qu, *Materials Today*, **2013**, *16*, 433-442.

[5] Q. Liu, B. Guo, Z. Rao, B. Zhang, J. R. Gong, *Nano Lett.*, **2013**, *13*, 2436–2441.

[6] X. Li, S. P. Lau, L. Tang, R. Ji, P. Yang, *J. Mater. Chem. C*, **2013**, *1*, 7308-7313.

[7] R. Justin, K. Tao, S. Román, D. Chen, Y. Xu, X. Geng, I. M. Ross, R. T. Grant, A. Pearson, G. Zhou, S. MacNeil, K. Sun, B. Chen, *Carbon*, **2016**, *97*, 54-70.

[8] R. Liu, D. Wu, X. Feng, K. Müllen, *J. Am. Chem. Soc.*, **2011**, *133*, 15221–15223.

[9] J. Peng, W. Gao, B. K. Gupta, Z. Liu, R. Romero-Aburto, L. Ge, L. Song, L. B. Alemany, X. Zhan, G. Gao, S. A. Vithayathil, B. A. Kaipparettu, A. A. Marti, T. Hayashi, J. J. Zhu, P. M. Ajayan, *Nano Lett.*, **2012**, *12*, 844−849.

[10] J. Lee, K. Kim, W. I. Park, B.-H. Kim, J. H. Park, T.-H. Kim, S. Bong, C.-H. Kim, G. S. Chae, M. Jun, Y. Hwang, Y. S. Jung, S. Jeon, *Nano Lett.*, **2012**, *12*, 6078.

[11] J. Rafiee, X. Mi, H. Gullapalli, A. V. Thomas, F. Yavari, Y. Shi, P.M. Ajayan, N. A. Koratkar, *Nat. Mater.* **2012**, *11*, 217−222.

[12] K.-S. Koh, J. Chin, J. Chia, C.-L. Chiang, *Micromachines* **2012**, *3*, 427-441.

[13] X. Song†, Y. Yang, J. Liu, H. Zhao, *Langmuir,* **2011**, 27, 1186–1191.

[14] S. I. Yoo, J.-H. Kwon, B.-H. Sohn, *J. Mater. Chem.*, **2007**, *17*, 2969-2975.

[15] Casaletto *et al*., *Surf. Interface Anal.* **2006**, *38*, 15–218.

[16] Y. Xue, X. Li, H. Li, W. Zhang, *Nat. Commun.* **2014**, *5*, 4348.

[17] A. C. Ferrari, D. M. Basko, *Nat. Nanotechno.* **2013**, *8*, 235–246.

[18] O. B. Shenderova, V. V. Zhirnov, D. W. Brenner, D. W., Critical Rev. Solid State and Mater. Sci. **2002**, *27***,** 227–356.

[19] A. Geim, *Science*, **2009**, *324***,** 1530–1534.

국문 초록

금을 도입한 마이셀을 에칭마스크로 사용한 화학증착그래핀에서 그래핀양자점의 제조

이 정 섭

화학부 고분자화학 전공

서울대학교 대학원

그래핀 양자점은 나노 크기의 그래핀 한장 또는 여러장으로서, 양자구속효과와 가장자리 효과로 인한 독특한 광학적, 기계적, 광전기적 특성을 가진다. 그래핀 양자점을 만들기 위해 잘 알려진 방법으로는 전자빔 식각, 화학적 합성, 산화그래핀의 환원, 그리고 수열방법 등이 있다. 이 연구의 목적은 이중블록 공중합체의 자기조립 현상을 이용하여 그래핀 양자점을 만드는 것이다. 이중블록 공중합체는 선택적 용매상에서 마이셀을 형성한다. 피리딘 블록에 금속 전구 물질이 도입된다는 점을 활용하기 위해 폴리스티렌-폴리-4-비닐피리딘 공중합체를 나노구조 제조에 이용하였다. 이중블록 공중합체 마이셀을 용매 증기로 풀림 처리하여, 실린더 나노구조를 다양한 기판 위에 제조하였다. 산소 플라즈마 공정을 통해 금속이 도입된 고분자 나노구조로부터 금속 나노구조를 만들었다. 이러한 방법으로 합성된 금속 나노입자를 식각 마스크로 이용하여 그래핀 양자점을 만들었다. 그래핀 양자점의 특성은 라만 분광법으로 확인하였다. 본 실험 결과에 의거하여, 잘 정의된

다양한 그래핀 나노구조를 반도체 분야의 응용에 쉽게 이용할 수 있을 것으로 본다.

주요어: 이중블록 공중합체, 자기조립, 그래핀 양자점, 라만 분광법
학 번: 2014-22409